DOI 10.5162/sensoren2024/D1.4

Modelling and Construction of Complex Shaped Polyvinyl Alcohol based Ultrasound Phantoms for Inverse Magnetomotive Ultrasound Imaging

Christian Heim[1], Christian M. Huber[2,3], Helmut Ermert[4], Ingrid Ullmann[3], Taimur Saleem[1], Stefan Lyer[2], and Stefan J. Rupitsch[1]
[1]Department of Microsystems Engineering (IMTEK), Laboratory for Electrical Instrumentation and Embedded Systems, University of Freiburg, Georges-Köhler-Allee 106, Germany
[2]Department of Otorhinolaryngology, Head and Neck Surgery, Section of Experimental Oncology and Nanomedicine (SEON), Professorship for AI-Controlled Nanomaterials (KINAM), Universitätsklinikum Erlangen, Glücksstraße 10a, Germany
[3]Institute of Microwaves and Photonics (LHFT), Friedrich-Alexander-Universität Erlangen-Nürnberg, Cauerstraße 9, Germany
[4]Department of Otorhinolaryngology, Head and Neck Surgery, Section of Experimental Oncology and Nanomedicine (SEON), Else Kröner-Fresenius-Stiftung-Professorship, Universitätsklinikum Erlangen, Glücksstraße 10a, Germany
{Christian.Heim; Stefan.Rupitsch; Taimur.Saleem}@imtek.uni-freiburg.de, {Christian.Huber; Stefan.Lyer}@uk-erlangen.de, {Helmur.Ermert; Ingrid.Ullmann}@fau.de

Abstract

With regard to the application in local cancer treatment, the inverse magnetomotive ultrasound (IMMUS) modality needs to be extended to 3D on complex shaped polyvinyl alcohol (PVA) phantoms. Our four basic construction elements can be combined step-by-step to manufacture such complex shaped phantoms. The construction of complex shaped ultrasound phantoms requires the four basic elements (i) molds, (ii) scattering material, (iii) layering process, and (iv) mechanical coupling between different parts of the phantom. In this contribution, we describe the construction elements in detail to show the trade-offs between the possible shapes and positioning of the encapsulated volumes and the production time.
Furthermore, since IMMUS requires knowledge of the mechanical parameters and the geometry of the target tumorous tissue, these parameters have to be determined during a magnetic drug targeting (MDT) therapy. The insertion of MDT therapy relevant amount of superparamagnetic iron oxide nanoparticles (SPIONs) does not significantly change the material properties. Therefore, quantitative ultrasound-based tissue characterization techniques (UTCT) such as shear wave elastography (SWE) or transient elastography (TE) can be used to characterize the target tumorous tissue once in advance of an MDT therapy. In this contribution, SWE and TE are exploited to determine shear wave velocity in PVA phantoms. Both methods show promising results for the determination of Young's modulus.

Keywords: Magnetic Drug Targeting, Magnetic Nanoparticles, Magnetomotive Ultrasound Imaging, Polyvinyl Alcohol Ultrasound Phantom, Ultrasound-based Material Characterization.

1. Motivation

A promising approach for local cancer treatment is MDT with SPIONs [1] in combination with an IMMUS based monitoring system [2, 3, 4, 5]. The idea of IMMUS is to compare the simulated magnetically induced tissue displacement with the sonographically determined real tissue displacement when a known alternating magnetic field is applied to set SPIONs in motion. However, IMMUS is currently limited to 2D only with pre-known material parameters and tumor geometry. These parameters of the tumorous tissue have to be determined individually during an MDT therapy. Our approach uses quantitative UTCTs such as SWE or TE. For the development and improvement of UTCTs, PVA based ultrasound phantoms can be used for baseline studies. PVA phantoms require a scattering material as an additive to make them similar to real tissue. However, such scattering material can change the material parameters of the PVA phantom. In this contribution, we describe an overview of important aspects of phantom manufacturing,

such as the processes involved in the manufacturing procedure, the principles for modelling PVA phantoms interspersed with SPIONs or microparticle scattering material, the construction of complex shaped phantoms as well as the experimental determination of the mechanical parameters Young's modulus, density and shear wave velocity.

2. Introduction

For the simulation part that is used in IMMUS, it could be shown that a linear-elastic mechanical model for PVA phantoms with three material parameters, i.e., 1st and 2nd Lamé parameters and density, is sufficient [4]. Furthermore, it was shown that a concentration of SPIONs of less than 4 mg/ml, which is relevant for an MDT therapy, has a very low influence of less than 0.3 % on the 1st and 2nd Lamé parameters [5]. The relative change in density is less than 0.5 %. These three material parameters can, therefore, be assumed to be effectively constant during an MDT therapy with varying particle distributions. Nevertheless, both the material parameters and the geometry of the tumorous tissue have to be measured individually during an MDT therapy. Consequently, tissue characterization techniques are required. One approach is to use quantitative UTCT such as TE or SWE. TE and SWE are clinically approved for use on humans. Both methods measure the velocity of propagating shear waves inside tissue. The relationship between shear wave velocity c_S, shear modulus G, Young's modulus E, density ρ and Poisson's ratio ν of an elastic isotropic solid can be expressed according to [6]

$$c_S = \sqrt{\frac{G}{\rho}} = \sqrt{\frac{E}{2(1+\nu)\rho}}\,. \qquad (1)$$

Poisson's ratio ν of human tissue and PVA phantoms can be assumed to be close to 0.5 and their density ρ approximately equals to the density of water ρ_{Water} = 1000 kg/m^3 [5, 7]. The influence of both parameters on c_S is shown in Fig. 1. It can be seen that the influence of Poisson's ratio ν is small compared to the influence of density ρ. Thus, variations of the Poisson's ratio could be neglected, but the density has to be determined for UTCTs.

For baseline studies on UTCTs, PVA phantoms can be used for the development and evaluation. UTCTs are quantitative methods and require a detailed understanding of used materials and manufacturing processes. A comprehensive review of PVA phantoms can be found in [8]. The density ρ of PVA phantoms can be determined exploiting Archimedes principle [9]. Young's modulus E can be determined using tensile-compression tests, which are well known in material testing. Results from literature can be found in [7, 10, 11]. Both methods can be applied on a disassembled reference phantoms manufactured in parallel to analyze individual parts.

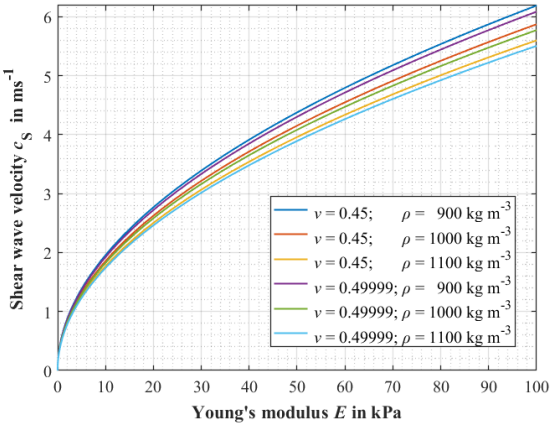

Fig. 1: Relationship between shear wave velocity c_S and Young's modulus E for different Poisson's ratios ν and densities ρ.

3. Freeze/Thaw Manufacturing Process for PVA Phantoms with Scattering Material

The manufacturing process involves four sequential steps for PVA phantoms. The basic ingredients are deionized water and polyvinyl alcohol powder. Firstly, a viscous gel is prepared by mixing (10–35) wt.% PVA powder with deionized water under continuous stirring and heating at about 80 °C. The final gel typically includes air inclusions and can be degassed using a bell jar. Secondly, a scattering material can be added to the gel. Particle sizes of about (60–100) µm increase the echogenicity as shown in Fig. 3 and Fig. 4. Rotation of the gel at a frequency of approximately 1 Hz may be required during the first freezing cycle to achieve uniform distribution of the scattering material. Thirdly, the gel is poured into a mold and completely packed with foil to prevent it from dehydrating during freezing and thawing. In the last step, the freeze/thaw method with multiple cycles is applied to harden the gel. A cycle consists of freezing the gel at a low temperature (e.g., -25 °C) and thawing at room temperature (e.g., 25 °C) for several hours. Freezing the gel results in the formation of ice, which causes entanglement and hydrogen bonding of the PVA chains. This kind of hardening is time, rate and temperature dependent [8]. The time required to completely freeze and thaw a complex phantom can be determined by

measuring the temperature over time with a thermocouple placed at the position furthest from the surfaces, e.g., the center of mass. After thawing the frozen gel, the melted ice leaves pores and the PVA chains remain in a stable three-dimensional arrangement.
Scanning electron microscope (SEM) images of 10 wt.% PVA phantoms with different numbers of freeze/thaw cycles are shown in [8, 11]. The resulting compression moduli of PVA phantoms with different wt.% PVA and different number of freeze/thaw cycles are shown in [10], which can be used as a reference for simple shaped phantoms. However, the mechanical parameters of complex shaped phantoms are decisive for UTCTs. The mechanical parameters are sensitive to the individual manufacturing process and should, therefore, be determined individually for each phantom.
The coupling and movement of interspersed nano- or microparticles due to pores within a PVA phantom needs to be investigated and should be taken into account when analyzing unexpected behavior.

4. Modelling Material Properties of PVA Phantoms

Scattering material such as microparticles can change the material properties. Therefore, a theoretical modelling to determine this change is necessary to apply Eq. (1). Hashin-Shtrikman boundaries are well known equations to model upper and lower bounds for the elastic moduli such as shear modulus G for a two-phase composite. A detailed description can be found in [5]. For isotropic PVA phantoms with uniform distributed iron nano- or microparticles, the lower bound G_{LB} reads as

$$G_{\mathrm{LB}} = G_1 + \frac{x}{(G_2 - G_1)^{-1} + 2(1-x)(5G_1)^{-1}}\,, \quad (2)$$

where x is the volume fraction of the scattering material, G_1 is the shear modulus of the PVA phantom, and G_2 is the shear modulus of the scattering material. Together with the relationship

$$G_i = \frac{E_i}{2(1+\nu)} \quad (3)$$

between shear modulus G and Young's modulus E, the lower bound G_{LB} can be calculated from various material properties of the scattering material.
According to Eq. (1), the change in density ρ has to be known as well to determine the shear wave velocity c_{S}. The resulting density ρ_{Res} can be modelled with

$$\rho_{\mathrm{Res}} = (1-x)\rho_1 + x\rho_2\,, \quad (4)$$

where x is the volume fraction of the scattering material. ρ_1 is the density of the PVA phantom and ρ_2 is the density of the scattering material. Fig. 2 shows the theoretical lower bound for the change in shear wave velocity c_{S} relative to the MDT therapy relevant amount of SPIONs using Eq. (1) to Eq. (4).

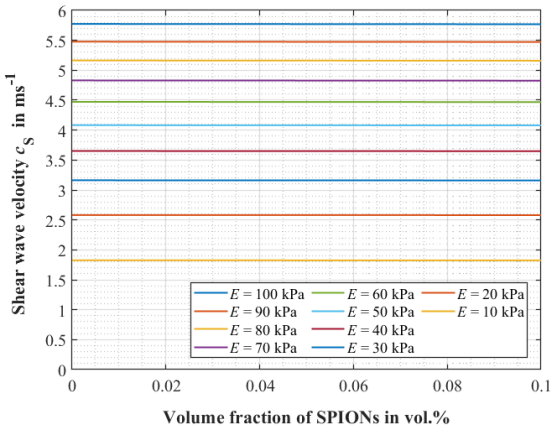

Fig. 2: Relationship between shear wave velocity c_{S} and volume fraction x of SPIONs for different Young's moduli E of the PVA phantom (PP). Used parameters: E_{SPION} = 100 GPa; ν_{SPION} = 0.25; ρ_{SPION} = 5200 kg/m^3; ν_{PP} = 0.49999; ρ_{PP} = 1000 kg/m^3 [5].

The theoretical relative change is about 0.1 %. Since Hashin-Shtrikman is a bound, an experiment was performed to check closeness to the lower bound. To measure shear wave velocity c_{S}, SWE was exploited with an ultrasound scanner (Siemens Acuson S2000; 9L4; 8 MHz; Virtual Touch Tissue Quantification). The measured shear wave velocities c_{S} are summarized in Tab. 1.

Tab. 1: SWE-based measurements of shear wave velocities c_S of two PVA phantoms (10 wt.%; 2 freeze/thaw cycles) with no and SPIONs interspersed inclusion, respectively.

Inclusion	c_{S} in ms^{-1}
No	4.6 ± 0.7
4 mg/ml SPIONs	4.5 ± 0.6

No significant change for c_{S} could be observed in the SPIONs interspersed volume. Therefore, the shear wave velocity c_{S} can be assumed to be constant during an MDT therapy. Nevertheless, a comprehensive study is required to verify the model for higher volume fractions and for different scattering materials.

5. Construction Elements for Manufacturing of PVA Phantoms

The construction of complex shaped ultrasound phantoms requires the four basic elements (i) molds, (ii) scattering material, (iii) layering process, and (iv) mechanical coupling between different parts of the phantom.

Molds define the final shape of the hardened gel and have a direct influence on the material parameters. Different molds, i.e., different materials with different thicknesses, used in the same freeze/thaw process could result in different material properties due to different temperature profiles for the hardening process. A mold has to deal with the increase of volume due to icing of water. It is, therefore, advisable to include an expansion volume. A foil can be used to encapsulate the gel to allow rotation, prevent dehydration and provide expansion volume. Molds of any shape can be produced using 3D printing technology.

Scattering materials are needed as an additive to the PVA to make phantoms similar to real tissue. UTCTs track the propagation of shear waves by analyzing the movement of tissue based on the speckle pattern created by scatters in biological tissue. Possible scattering material for PVA phantoms are nanoparticles, microparticles or µm-wires.

A layering process is required to manufacture phantoms that cannot be hardened at once, e.g., a complete encapsulated and mechanical coupled inner volume such as a tumor. The layering process is based on the continuation of the physical crosslinking process after new gel has been added to already iced gel within the same freezing phase of a cycle. With this approach, even more complex shaped phantoms can be manufactured. It should be mentioned that the material parameters can vary slightly between layers due to different local temperature profile.

Mechanical coupling between different phantoms or with other materials is important to perform experiments with the phantoms. The type of coupling principle depends on the experimental setup and whether the coupling should be reversed after the experiment. The simplest type is gluing with superglue or PVA gel, but this cannot be reversed. Superglue is well suited for an immovable and permanent bond with materials such as iron, aluminum, plastic, etc., while PVA gel is well suited for flexible bonds between PVA phantoms. Another type is mechanical fixation with customized phantom geometries such as screw holes or threads. This can be reversed, but additional phantom material is required. As the phantom also requires an immovable coupling that can be reversed, a vacuum holder can be used.

6. Sample Manufacturing Processes of Complex Shaped Phantoms for UTCT and IMMUS

The following two manufacturing processes explain the four basic construction elements of how a complex shaped PVA phantom can be manufactured for UTCT and IMMUS. For reasons of clarity, only the inner volume was interspersed with scattering material. Fig. 3 shows a manufacturing process for a phantom with an inner cube with additional scattering material.

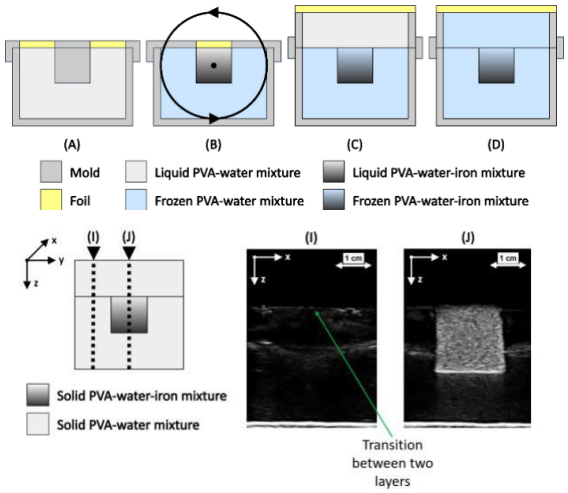

Fig. 3: Side view of steps for the layered manufacturing process (A)–(D) with mechanical coupling, combined with scattering material in the inner cube to increase echogenicity and B-mode images at positions (I) and (J).

The inner cube is completely enclosed and mechanically coupled to its surrounding. This is achieved by continuing the physical crosslinking process after new gel has been added to the iced gel. The entire phantom should, therefore, feature approximately the same material parameters. The material parameters of the inner cube, however, are changed by the scattering material. Rotation at a frequency of around 1 Hz is required in the first freezing phase to achieve uniform distribution of the scattering material. The main advantage is the reproducibility of the position and shape of the inner volume and the main disadvantage is the manufacturing time.

Fig. 4 shows a manufacturing process for a phantom with a harder inner cube interspersed with scattering material. The inner cube is pre-hardened with µm-wires for later fixation and then encapsulated. The main advantage of this manufacturing process is the full mechanical

coupling of a pre-harded inner volume with arbitrary shape, the main disadvantage is that it is not easy to reproduce the position and shape of the inner volume.

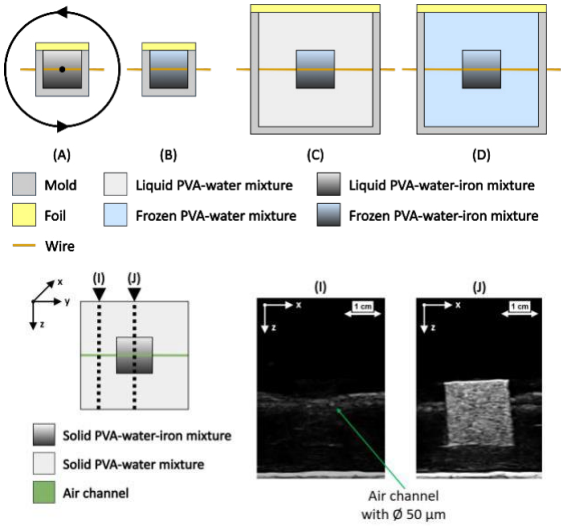

Fig. 4: Side view of the steps for coupling process (A)–(D) with mechanical coupling of different hard parts, combined with scattering material in the inner cube and B-mode images at positions (I) and (J).

7. Determining Young's Modulus with Transient Elastography

TE is based on sonographic time tracking of a mechanical shear wave propagating through the investigated specimen, in our case a PVA phantom with iron microparticles [9]. Slope evaluation of the first wave front in M-mode imaging was exploited for this purpose with an ultrasound scanner (Ultrasonix SonixTouch; L9-4; 6.6 MHz). Fig. 5 shows a schematic representation of the utilized experimental setup.

The PVA phantom consists of 10 wt.% PVA (DuPont Elvanol 71-30) and deionized water. 10 wt.% iron microparticles (Metallpulver 24 CUT150) were added as scattering material. The mixture was hardened by the freeze-thaw method with two cycles at -25 °C for 6 h and 25 °C for 6 h.

To excite a shear wave in the phantom, the phantom was glued to a holder and a mechanical impulse was generated by a plate mounted on an electrodynamic shaker (Tira S504). The shear wave was tracked by the ultrasound scanner on the opposite side of the phantom. Density ρ was determined before gluing using Archimedes principle with a laboratory balance (Denver TP-3002). Young's modulus E was determined using tensile-compression testing machine (Zwick/Roell ZMART.PRO). In order to have similar conditions as for the TE measurements, the phantom was placed in the mold for the compression test. All determined parameters are summarized in Tab. 2.

Tab. 2: Measured material parameters of a 10 wt.% PVA phantom (2 freeze/thaw cycles) with 10 wt.% iron microparticles scattering material.

Parameter	Value
E	(77.3 ± 3.9) kPa
ρ	(1063.1 ± 3.7) kg/m^3
c_S	(4.8 ± 0.2) ms^{-1}

No significant change for c_S could be observed in a 10 wt.% PVA phantom interspersed with 10 wt.% scattering material. The change in density ρ is 6.3 % relative to the density of water ρ_{Water}. The density ρ is, therefore, a parameter, which has to be determined for the quantitative determination of the Young's modulus E exploiting UTCTs. Assuming a Poisson's ratio ν = 0.5, the values from Tab. 2 show a reasonable relationship according to Eq. (1). Thus, SWE and TE can be used as quantitative methods to determine the Young's modulus E needed for the simulation part of IMMUS.

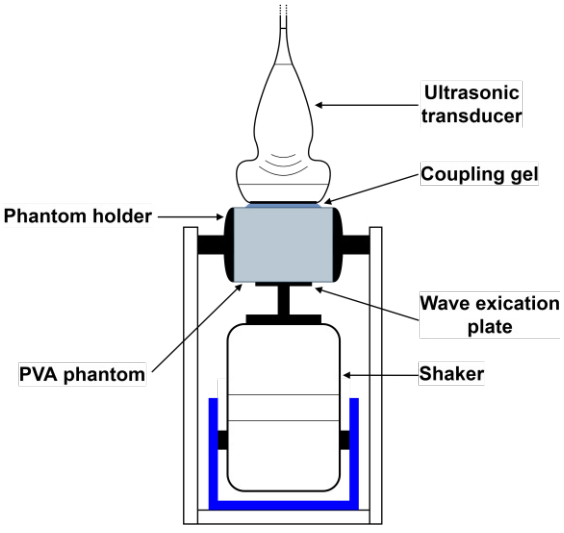

Fig. 5: Experimental setup to excite and measure shear waves inside a PVA phantom. The shear wave is excited by the wave excitation plate and propagates from the bottom of the phantom to the top.

8. Conclusions

The IMMUS modality needs to be extended to 3D on complex shaped PVA phantoms. Since IMMUS requires knowledge of the 1st and 2nd

Lamé parameter, the density, and the geometry of the target tumorous tissue, these parameters have to be determined during an MDT therapy. As SPIONs have very low influence on the material parameters, the material parameters and the geometry only need to be characterized once before applying an IMMUS monitored MDT therapy. SWE and TE show promising results for the determination of Young's modulus and can, therefore, be applied for this purpose. In order to use SWE and TE as a quantitative method for the determination of Young's modulus, it is necessary to know the density locally. For complex shaped PVA phantoms, local density and other parameters can be determined using a disassembled reference phantom manufactured in parallel. Poisson's ratio can be assumed to be constant and close to 0.5.
The construction of complex shaped PVA phantoms requires only the four elements (i) molds, (ii) scattering material, (iii) layering process, and (iv) mechanical coupling between different parts of the phantom. All the elements can be combined step-by-step to manufacture complex shaped phantoms. Trade-offs have to be made between the possible shapes, the positioning of the encapsulated volumes, the production time and the mechanical fixation.

9. Outlook

In future contributions, our research will focus on automated 3D-SWE and 3D-TE for both isotropic and anisotropic complex shaped PVA phantoms to determine the Young's modulus distribution together with the tumor geometry in order to create an accurate simulation model of the target tumor tissue for the IMMUS modality.
Furthermore, as the density distribution within a PVA phantom or biological tissue is required for UTCTs, an ultrasound-based characterization method will be investigated.

Acknowledgment

The authors gratefully acknowledge the financial support of the Deutsche Forschungsgemeinschaft (DFG) - project number 452821018.

References

[1] R. Tietze, S. Lyer, S. Dürr, T. Struffert, T. Engelhorn, M. Schwarz, et al. “Efficient Drug-Delivery Using Magnetic Nanoparticles - Biodistribution and Therapeutic Effects in Tumour Bearing Rabbits,” *Nanomedicine* 9(7), 961–971 (2013); doi: 10.1016/j.nano.2013.05.001

[2] M. Fink, S. J. Rupitsch, S. Lyer, C. Alexiou, H. Ermert, “Quantitative Imaging of the Iron-Oxide Nanoparticle-Concentration for Magnetic Drug Targeting Employing Inverse Magnetomotive Ultrasound,” *Current Directions in Biomedical Engineering* 5(1), 417–420 (2019); doi: 10.1515/cdbme-2019-0105

[3] M. Fink, S. J. Rupitsch, S. Lyer, C. Alexiou, H. Ermert, “An Enhanced Magnetomotive Ultrasound Algorithm to Quantitatively Estimate the Concentration of Iron-Oxide Nanoparticles in Perfused Tissue for Magnetic Drug Targeting,” *IEEE International Ultrasonics Symposium (IUS)*, 1407–1409 (2019); doi: 10.1109/ULTSYM.2019.8925977

[4] M. Fink, S. J. Rupitsch, S. Lyer, H. Ermert, “Quantitative Determination of Local Density of Iron Oxide Nanoparticles Used for Drug Targeting Employing Inverse Magnetomotive Ultrasound,” *IEEE Transactions on Ultrasonics, Ferroelectrics, and Frequency Control* 68(7), 2482–2495 (2021); doi: 10.1109/tuffc.2021.3068791

[5] M. Fink, “Ultraschallbasierte Bestimmung der räumlichen Verteilung magnetischer Nanopartikel bei Magnetic-Drug-Targeting-Anwendungen,” dissertation, Faculty of Engineering, Friedrich-Alexander-Universität Erlangen-Nürnberg, Germany, 2023; doi: 10.25593/open-fau-104

[6] S. J. Rupitsch, “Piezoelectric Sensors and Actuators – Fundamentals and Applications,” Springer, Germany, 2019; doi: 10.1007/978-3-662-57534-5

[7] J. Fromageau, J. Gennisson, C. Schmitt, R. L. Maurice, R. Mongrain, G. Cloutier, “Estimation of polyvinyl alcohol cryogel mechanical properties with four ultrasound elastography methods and comparison with gold standard testings,” *IEEE Transactions on Ultrasonics, Ferroelectrics, and Frequency Control* 54(3), 498–509 (2007); doi: 10.1109/TUFFC.2007.273

[8] H. Adelnia, R. Ensandoost, S. S. Moonshi, J. N. Gavgani, E. I. Vasafi, H. T. Ta, “Freeze/thawed polyvinyl alcohol hydrogels: Present, past and future,” *European Polymer Journal* 164, 110974 (2022); doi: 10.1016/j.eurpolymj.2021.110974

[9] A. Baghani, H. Eskandari, S. Salcudean, R. Rohling, “Measurement of viscoelastic properties of tissue-mimicking material using longitudinal wave excitation,” *IEEE Transactions on Ultrasonics, Ferroelectrics, and Frequency Control* 56(7), 1405–1418 (2009); doi: 10.1109/TUFFC.2009.1196

[10] J. L. Holloway, A. M. Lowmanb, G. R. Palmese, “The role of crystallization and phase separation in the formation of physically cross-linked PVA hydrogels,” *Soft Matter* 9, 826–833 (2013); doi: 10.1039/c2sm26763b

[11] A. Sharma, S. G. Marapureddy, A. Paul, S. R. Bisht, M. Kakkar, P. Thareja, K. P. Mercado-Shekhar, “Characterizing Viscoelastic Polyvinyl Alcohol Phantoms for Ultrasound Elastography,” *Ultrasound in Medicine & Biology* 49(2), 497–511 (2023); doi: 10.1016/j.ultrasmedbio.2022.09.019